FRET measurements between small numbers of molecules identifies subtle changes in receptor interactions

FRET measurements between small numbers of molecules identifies subtle changes in receptor interactions

Serdar Özçelik,* Galya Orr,* Dehong Hu, Chii-Shiarng Chen, Haluk Resat, Greg S. Harms[‡], Lee K. Opresko, H. Steven Wiley and Steven D. Colson.
Chemical and Biological Sciences Divisions, Pacific Northwest National Laboratory, Richland, WA 99352, USA

Keywords: FRET, fluorescence, cells, dimerization, EGFR, HER2.

ABSTRACT

Overexpression of HER2 alters the cellular behavior of EGF receptor (EGFR) and itself, with great implications on cell fate. To understand the molecular interactions underlying these alterations, we quantified the association between the two receptors by looking at efficiency changes in fluorescence resonance energy transfer (FRET) between a small number of molecules at the membrane of living cells. Human mammary epithelial (HME) cells expressing varying degrees of HER2 were studied, to identify and compare the degree of receptors interactions as a function of HER2 overexpression. A high resolution wide-field laser microscope combined with a high sensitivity cooled CCD camera was used to capture simultaneously donor and acceptor emissions. Alternating between green and red lasers every 80 msec, donor, FRET, and acceptor images were acquired and were used to calculate FRET efficiency. Automated image analysis was developed to create FRET efficiency maps from overlapping donor, acceptor and FRET images, and derive FRET efficiency histograms to quantify receptor-receptor interactions pixel by pixel. This approach enabled us to detect subtle changes in the average distance between EGFR molecules, and between EGFR and HER2. We found pre-existing EGFR homoassociations, and EGFR-HER2 heteroassociations in cells overexpressing HER2, and identified the changes in these interactions with ligand stimulation. These observations demonstrate the power of FRET measurements between small numbers of molecules in identifying subtle changes in molecular interactions in living cell.

*Correspondence: G. Orr (galya.orr@pnl.gov, 509 376 9592); S. Ozcelik (serdar.ozcelik@pnl.gov, 509 376 4026).
[‡] Current address: Universität Würzburg, Rudolf-Virchow-Zentrum, Versbacherstr. 9, 97078 Würzburg, Germany.

1. INTRODUCTION

The dimerization of receptors in the plasma membrane is a common mechanism for controlling receptor activation, and the initiation of intracellular molecular cascades that in turn determine the fate of the cell. HER2 is an orphan receptor with no known ligand that depends on the association with other members of the ErbB family of receptors for its activation and internalization under normal conditions. Over-expression of HER2 causes profound changes in the cellular behavior of EGFR and the other family members as well as its own behavior, leading to cell transformation, and increased cell proliferation, migration and invasiveness.[1-4] To better understand the mechanisms underlying the cellular changes caused by HER2 over-expression, we looked for differences in EGFR hetero-association with HER2, and EGFR homo-association in human mammary ephithelial cells expressing varying degrees of HER2. Several tools are available for detecting receptor interactions in real-time in living-cells. One approach relies on complementation to gain enzymatic activity.[5] For example, the dimerization of EGFR after EGF binding was detected by fusing the receptor extracellular and transmembrane domains to weakly complementing β-galactosidase deletion mutants that could gain enzymatic activity only upon EGFR dimerization.[6] The main advantage of this approach is the amplification of the signal by the enzymatic reaction. Similarly, complementation has been used to gain enzymatic activity by dihydrofolate reductase (DHFR).[7] Using this approach, preexisting dimers of erhythropoietin receptor were identified by dimerization-induced complementation of designed fragments from DHFR.[8] When the fragments are fused to interacting proteins, they reassemble and bind the fluorescein-conjugated inhibitor methotrexate, which in turn is retained in the cell. The

Multiphoton Microscopy in the Biomedical Sciences IV, edited by Ammasi Periasamy, Peter T. C. So, Proceedings of SPIE Vol. 5323 (SPIE, Bellingham, WA, 2004) · 1605-7422/04/$15 · doi: 10.1117/12.536770

presence of interacting receptors is then detected by fluorescein emission. A relatively new approach for detecting molecular interactions within living cells utilizes dyes that change their emission spectra and intensity with changes in the local environment, assumed to occur with protein binding and dissociation. The most prevalent approach for detecting receptor dimerization within living cells is FRET. FRET efficiency is proportional to the sixth power of the distance between two fluorescent molecules, leading to relatively large changes in FRET efficiency with subtle changes (Å resolution) in the distance between the two dyes. This property makes FRET an excellent reporter of molecular interactions, which occur within ~ 100 Å, and their dynamic changes in real time. FRET can be detected and measured in several ways. Donor fluorescence lifetime imaging reports the decrease in the donor lifetime as a result of the transfer of energy.[9] This approach relies on pulsed lasers and measurements of photons arrival time relative to the laser pulse. The advantage of this approach is its independence of concentrations. Another common way of measuring FRET is comparing the intensity and photobleaching time of the donor emission before and after acceptor photobleaching (or in the presence or absence of the acceptor). The two approaches described above do not rely on acceptor emission for FRET calculation. One of the most quantitatively accurate approaches to measure FRET relies on both donor and acceptor simultaneous emissions with donor excitation. FRET is then calculated by the ratio between acceptor and donor emissions. In cases where the emissions are acquired with CCD cameras and not by flow cytometry for example, this approach also provides the ability to ensure that FRET signals originate from acceptor molecules, pixel by pixel. FRET has already been used to unravel the molecular interactions of EGFR and HER2, mostly identifying preexisting hetero- and homo-associations between the two receptors. Using both donor fluorescence lifetime and donor photobleaching time, pre-oligomerized EGFR was detected by FRET occurrence between two fluorescent ligands in quiescent A431 cells at 4° C.[10] Recently, FRET was used to show that membrane microdomains with a high density of HER2 molecules contained high degrees of HER2 homo-associations.[11] Considerable homo-association of HER2 and hetero-association of HER2 with EGFR were also detected using FRET in unstimulated breast tumor cells.[12] HER2 homo-association was enhanced by EGF in suspended cells but not in attached cells. Naturally, FRET detection and quantification is limited by the conventional fluorescence microscopy and fluorescence detection sensitivity. Recent technical advances in fluorescence imaging and spectroscopy have led to the emerging field of single-molecule fluorescence imaging and spectroscopy.[13-15] Using single-molecule FRET it was possible for example, to detect the number of fluorescent biotin molecules that bind to individual streptavidin receptors.[16] Here we engage the technology that is used for single-molecule fluorescence imaging to identify and quantify FRET occurrence between a small number of receptors within a small area of the membrane of living HME cells. Matlab routines were developed for automated FRET detection and quantification, providing the consistency and precision needed to analyze hundreds of cells. We have assembled a molecular model from the available crystal structures of EGFR and HER2 to simulate the complexes that are formed between the receptors while bound by the labeled Fab fragments. The molecular models allowed us to predict the distance between the fluorescent dyes, and to confirm the existence of receptor associations delineated from FRET efficiency measurements. We were able to detect pre-existing EGFR-HER2 hetero- and homo-associations in living HME cells expressing varying degrees of HER2 molecules, in real time. These observations demonstrate the power of applying high sensitivity fluorescence imaging in detecting subtle FRET signals and quantify their changes in response to biological stimulations in living cells.

2. METHODOLOGY

2.1. High sensitivity fluorescence microscopy for simultaneous acquisition of donor and acceptor emissions: The microscope configuration for simultaneous acquisition of donor and acceptor emissions is shown in figure 1. An inverted microscope (Zeiss, axiovert 200) equipped with a 100x oil-immersion objective (Zeiss, Plan-Apochromat, N.A.=1.4) was used. A green laser (Nd:YAG Verdi V-10, Coherent) was used to excite the donor at 532 nm, and a red laser (dye laser CR-599, Coherent) was used to excite the acceptor at 632 nm. The laser beams were coupled by a fiber coupler to the microscope to gain precise overlap between the two beams at the focal plane. The excitation polarization of the lasers was controlled by $\lambda/4$ and $\lambda/2$ wave-plates (Meadowlark Optics). The diameter of the beam at the focal plane was set to 8.0 μm^2 for the green laser, and 5 μm^2 for the red laser by a lens set in front of the epi-fluorescence port. The illumination intensities were adjusted to 7 kW/cm^2 for the green and red lasers. Ultrafast shutters, controlled by the CCD controller, were set in front of the laser beams, allowing 5 ms laser exposures at 12 Hz. The shutters allowed toggling between the two lasers while acquiring both donor and

acceptor emissions. A custom built dual dichroic beam-splitter and band-pass emission filters (Chroma Technology) were used to distinguish scattered light from fluorescence emission. Images of donor and acceptor emissions were acquired simultaneously on two distinguished areas of the CCD chip by a custom built dichroic wedge mirror (1^o angle, centered at 630 nm, Chroma Technology) that was placed at the bottom port of the microscope. The dual images were then refocused by an achromatic lens onto a back-illuminated cooled CCD camera (Roper Scientific, Spec-10 1340x400B) with 90% quantum efficiency at single-molecule fluorescence sensitivity.

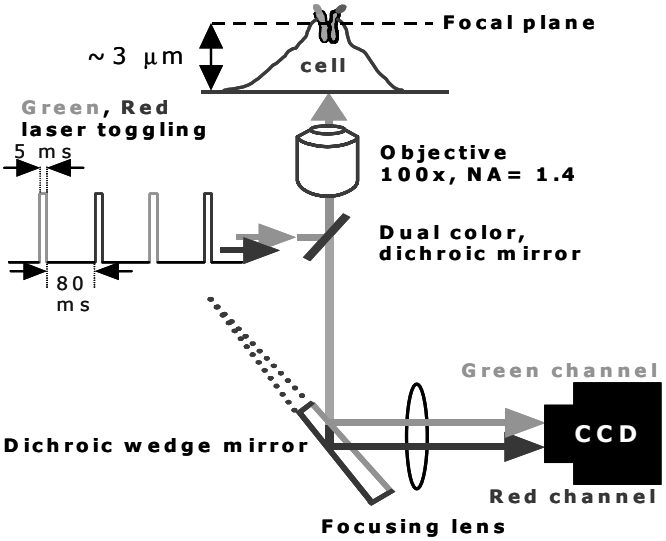

Figure 1: The experimental setup for FRET imaging, using a dichroic wedge mirror developed by Cognet et al.,[17] for simultaneous acquisition of donor and acceptor emissions.

The detection efficiency of the setup (η) was calculated using equation (1).

$$\eta = Q_{CCD} \times \eta_{NA} \times T_{obj} \times T_{filter} \times T_{lens} \times T_{window} \times R_{wedge} \qquad (1)$$

Q_{CCD} and η_{NA} are respectively the quantum efficiency of the CCD and the collection efficiency of objective. T_{obj} , T_{filter} , T_{lens} , and T_{window} are the transmissivity coefficients of the objective, filters, lens and window in front of CCD, respectively. R_{wedge} is the reflectivity of the wedge mirror. The efficiencies were 0.085 for for the alexa Fluor-546 (Molecular Probes, Eugene, OR) in the donor channel and 0.065 for the alexa Fluor-647 in the acceptor channel.

The crosstalk (the spectral bleed-through) between the two channels was estimated by measuring the spectra of the filters, knowing the spectral efficiency of the CCD, and calculating the total detection efficiency of the setup. We found that the crosstalk coefficient for the donor (alexa Fluor-546) in the red channel (the acceptor channel) was less than 0.10, and less than 0.03 for the acceptor (alexa Fluor-647) in the green channel (the donor channel). The estimated values were experimentally confirmed by measuring donor emission in the absence of acceptor, and acceptor emission in the absence of the donor, in all channels.

2.2. HME cell-lines, Fab fragments, and labeling: The parent, 184A1, cell-line was a kind gift from Martha Stampfer (LLNL, Berkeley, CA). This cell-line was used to create HER2 overexpressing cell-lines by retroviral transduction, as is described elsewhere.[18,19] The parent cells were grown in DFCI-1 medium supplemented with 12.5 ng/ml EGF, and HER2 overexpressing cells were grown in the same medium with the addition of 100 µl/ml G418-sulfate. All cell-lines were grown in 30 mm tissue-culture plates with a glass coverslip bottom. 13A9 mAb

against EGFR (binds to domain III), and 7C2 Fab fragment against HER2 (binds at domain I), were generous gifts from Genentech, Inc. Fab fragments of 13A9 mAb were generated using agaros Bead-immobilized papain (Pierce Inc., Rockford. IL). The Fab fragments were labeled with alexa fluor-546 or alexa fluor-647 using NHS ester derivatives of the dyes in PBS at pH 8.0-10.0. The degree of labeling (D.O.L.) was calculated according to Lambert-Beer Law as described in Molecular Probes protocols, and was estimated to be 1~1.2 for all labeled Fab fragments used in this study. These values were confirmed by single-molecule fluorescence measurements as is described below.

2.3. D.O.L measurements by single-molecule fluorescence microscopy: The intensities of single fluorophores spin-coated on coverslips with concentration of 100 pM were determined by the counts of the individual, diffraction limited, hotspots observed under our experimental conditions. The hotspots were regarded as single-molecules if they are photobleached in a single step. Intensity histograms (figure 2), generated from hundreds of hotspots indicated the expected photon-counts of single fluorophores under our experimental parameters. Intensity histograms of Fab fragments labeled with the fluorophores were generated as described above for the fluorophores alone, identifying the distribution of the degree of labeling of single Fab fragments. We found that more than 95% of the fab fragments were labeled with one fluorophore, confirming D.O.L. = 1.0.

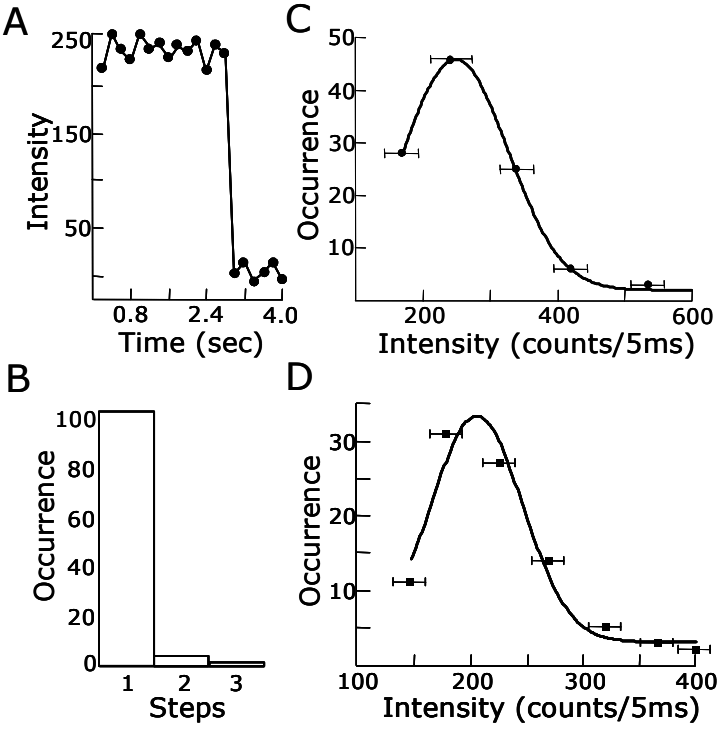

Figure 2: (A) Single-step photobleaching of the donor (Alexa Fluor-546), a signature of single-molecule fluorescence. (B) D.O.L. of 7C2 (Fab)-Alexa Fluor-546, as determined by counting the number of steps that took for the fluorescence spot to completely disappear. (C) The fluorescence intensity distribution of the donor, and the acceptor (D) as measured from the labeled Fab fragments spin-coated on coverslips.

2.4. FRET experiments: Cells were grown to 70% confluence and were brought to quiescence by overnight incubation in minimal DFCI-1 (without sodium bicarbonate, EGF, bovine pituitary extract or fetal bovine serum), containing 1% BSA. The cells were incubated at 37 ^{o}C in an air incubator. Receptor labeling was carried out by 30 min incubation on ice with 1:2 mol ratio of donor and acceptor molecules in the above minimal medium. To quantify EGFR homoassociation, 13A9 Fab fragments labeled with alexa fluor-546 (alexa fluor-647) at 0.250 (0.500) nM concentration each, were used. To quantify EGFR – HER2 heteroassociation, 7C2 Fab fragments labeled with alexa fluor-546 and 13A9 Fab fragments labeled with alexa fluor-647 at 0.250 and 0.500 nM

concentrations respectively, were used. FRET measurements were carried out at room temperature, while focusing at the upper cell membrane, on an area of 8.0 μm^2. To image the interactions in the presence of saturating concentrations of the ligand, recombinant EGF (Sigma) was added, to give a final concentration of 200 nM.

2.5. FRET image analysis: Matlab codes were written for all image analyses. Three channels were considered: the DONOR channel (donor emission with green excitation), the ACCEPTOR channel (acceptor emission with red excitation), and the FRET channel (acceptor emission with green excitation) (figure 3A). Since the optical resolution of the setup (~300 nm) is larger than the pixel size (100 nm), the intensity at each pixel was averaged using 3x3 grid around each pixel, where

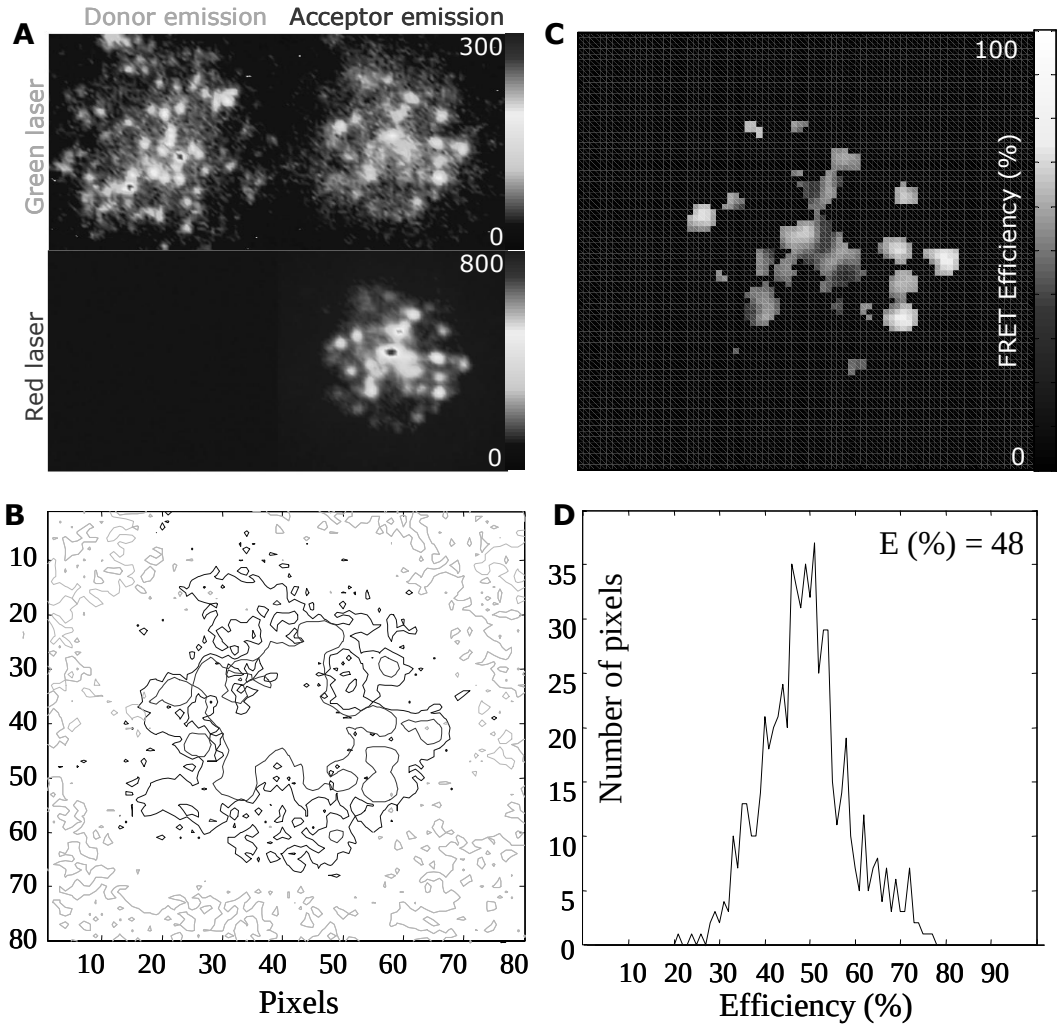

Figure 3: FRET image analysis, see text for details.

the central pixel, the four surrounding pixels sharing an edge with the center, and the four diagonally neighboring pixels contributed 40%, 40%, and 20% to the averages, respectively. The ACCEPTOR intensities were used to define a cutoff value to create a binary mask. This was done to determine whether the signal in the FRET channel at a given pixel is due to energy transfer and not due to autofluorescence, as FRET should occur only at locations where acceptor molecules are found. The FRET intensities were used to define a cutoff value based on reasonable noise background levels in the FRET images. Only the pixels that have ACCEPTOR and FRET intensities above

their respective cutoff levels were included in the FRET efficiency analysis. Contour maps of the three images were generated and superimposed to identify the overlapping signals (figure 3B). Signals in the FRET channel were considered, only if they overlapped with signals in the ACCEPTOR channel. Background counts were subtracted from the image using a background correction image. Photon-counts were calculated for each pixel, representing 0.1 μm^2 at the cell membrane, in each of the three channels, and the intensities were corrected for the spectral crosstalk discussed earlier. FRET efficiency (E) was then calculated pixel-by pixel (figure 3C) using equation 2, where I is the fluorescence intensity in the respective channels (indicated in parentheses), β (0.10) and α (0.03) are the percentage spectral bleed-through in the DONOR and the ACCEPTOR channels respectivley, and γ (0.82) is the ratio of the quantum yields of the two dyes.

$$Eff(\%) = 100 * \frac{\mathrm{I(FRET)} - \beta * \mathrm{I(DONOR)} - \alpha * \mathrm{I(ACCEPTOR)}}{\mathrm{I(FRET)} + \gamma * \mathrm{I(DONOR)}} \qquad (2)$$

A histogram of FRET efficiencies versus number of pixels was generated for each cell (figure 3D), and the weighted-average of the distribution was taken as the average FRET efficiency for the cell. This value was calculated for ~ 200 cells per cell-line, and the average of all cells in each cell-line was then calculated and designated as the FRET efficiency of the cell-line. FRET efficiency maps were then used to derive proximity maps by calculating the distance (R) in Å between the two fluorophores for each pixel. Equation 3 was used to calculate R, where R_0 is the Förster distance (74 Å in our case).

$$\frac{R}{R_o} = (E^{-1} - 1)^{1/6} \qquad (3)$$

To verify the expected anti-correlation between DONOR and FRET intensities, as energy is transferred from the donor to the acceptor molecules, normalized intensities in each channel were plotted for each pixel in an image (figure 4).

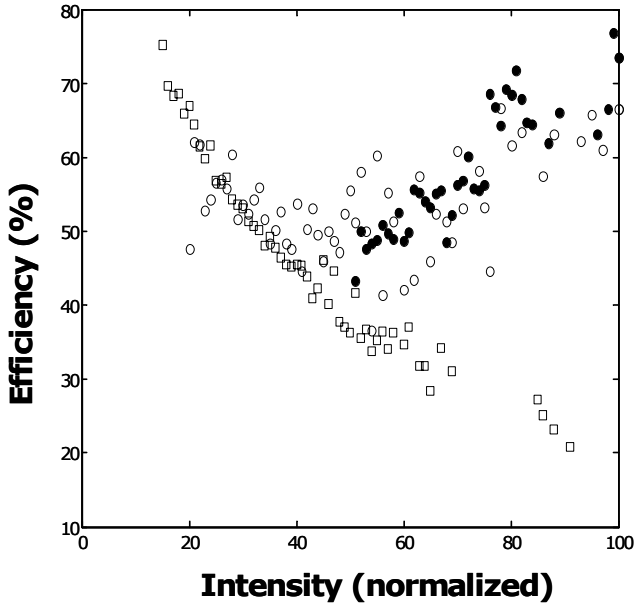

Figure 4: (A) Anticorrelation between the intensities of the donor (open squares) and the acceptor in the FRET channel (closed circles), confirms the transfer of energy.

3. RESULTS

In this work we engage the technology that is used for single-molecule fluorescence imaging to identify and quantify FRET occurrence between small numbers of receptors within a small area of the membrane of living HME cells. By toggling between two lasers to excite the donor and the acceptor, and using the optical configuration that was developed by Schmidt and colleagues,[17] we acquire simultaneously the emissions of the donor and the acceptor on two separate areas of the CCD chip. FRET efficiency is then calculated by the intensity ratio between the donor and acceptor emissions with donor excitation. Images of 8 μm^2 cell membrane areas were acquired from more than 200 cells per cell line, and FRET efficiency distributions for these cells were generated. Figure 5A shows an example of the FRET efficiency distribution for the HME cell-line that was engineered to express high levels of HER2, describing the interaction between EGFR and HER2. Clear hetero-associations were detected in unstimulated cells, and an increase in FRET efficiency was observed with EGF stimulation. We have developed Matlab routines for automated FRET detection and quantification, providing the consistency needed to analyze hundreds of cells. EGFR and HER2 have been tagged with labeled Fab fragments of 13A9 and 7C2 antibodies (Genentech Inc.) respectively. Since the antibody epitops are known, we took advantage of the recently achieved crystal structures [20-24] of EGFR and HER2 to create a molecular model of the dimers in complex with the labeled Fab fragments. We used Insight2 to simulate the complexes that are formed between EGFR-EGFR and EGFR-HER2 while bound by the labeled Fab fragments (figure 5B). The molecular models allowed us to measure the expected distance between the fluorescent dyes, and to confirm that the values of FRET efficiencies we observed, fall within the expected values delineated from the crystal structures. We were able to detect pre-existing EGFR-HER2 hetero- and homo-associations in living HME cells expressing varying degrees of HER2 molecules, in real time. These observations demonstrate the power of applying high sensitivity fluorescence imaging in detecting subtle FRET signals and quantify their changes in response to biological stimulations in living cells.

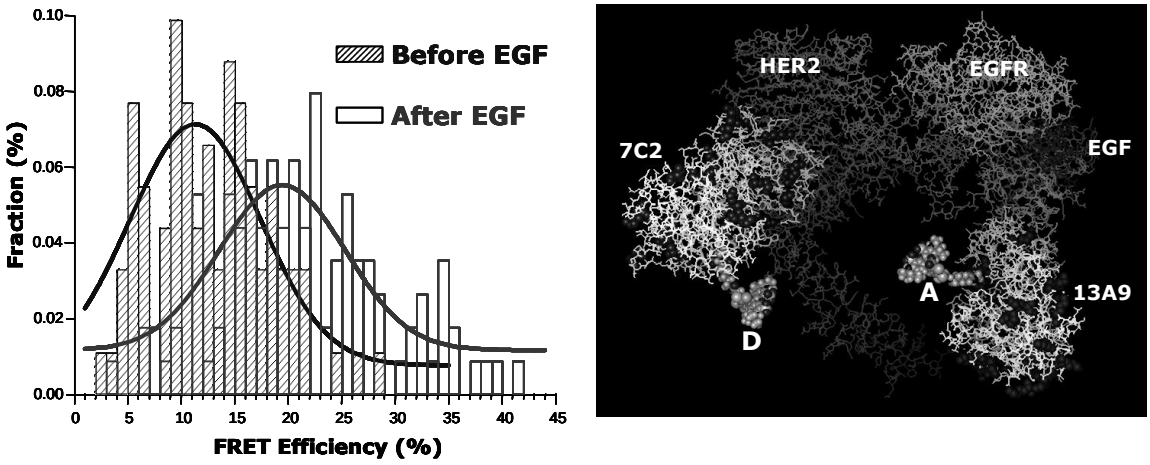

Figure 5: (A) FRET efficiency distribution describing the interaction of EGFR with HER2 in cells engineered to overexpress HER2. (B) The crystal structures of EGFR and HER2 in complex with the labeled Fab fragments, showing the expected distance between the two fluorescent dyes, D and A.

4. DISCUSSION

This work demonstrates the application of the technology used in single-molecule fluorescence imaging to identify molecular interactions between small numbers of receptors in the membrane of living cells, in real time.

This approach enabled us to image and resolve a small number of receptors (2-20 molecules), and to identify subtle FRET signals that were otherwise masked in high level, ensemble fluorescence measurements. The inevitable cross-talk between acceptor and donor excitation and emission channels was minimized here by dealing with a few fluorescent molecules, allowing the detection and precise calculation of the changes in FRET efficiency. FRET was detected using a unique setup that was designed to simultaneously capture the fluorescence emissions of the donor and the acceptor on two regions of the CCD camera, while toggling between two lasers. Toggling between donor and acceptor excitations allowed the simultaneous acquisition of donor and acceptor emissions with donor excitation, followed by acceptor emission with direct excitation. The three emission channels were then analyzed using automated Matlab routines to reliably and precisely identify the pixels containing FRET signals. FRET efficiency was calculated by the ratios of acceptor to donor emissions with donor excitation, an approach that provides a precise and reliable quantification of the interactions. This precision was further enhanced by the automated FRET analysis we have developed. EGFR and HER2 were tagged by labeled Fab fragments that were directed toward known regions in their extracellular domains. We took advantage of this knowledge, and the available crystal structures of the receptor to verify that the distance between the receptors, delineated from the FRET efficiencies we observed, fell within the expected distances in the crystal structures. The approach described above provides a sensitive and precise tool to identify molecular interactions and their subtle changes within living cells.

Acknowledgement: We thank Erich Vorpagel from the Molecular Sciences Computing and Visualization Facility at Pacific Northwest National Laboratory for assembling the molecular models and sharing his expertise. This work was supported by Pacific Northwest National Laboratory Directed Research and Development funds.

REFERENCES

1. P. P. Di Fiore, J. H. Pierce, M. H. Krause, O. Segatto, C. R. King, S. A. Aaronson, "erbB-2 is a potent oncogene when overexpressed in NIH/3T3 cells", *Science*, **237**, 178-182, 1987.
2. B. H. Brandt, A. Roetger, T. Dittmar, G. Nikolia, M. Seeling, A. Merschjann, J-R. Nofer, G. Dehmer-Moller, R. Junker, G. Assman, K. Zaenker, "c-erbB-2/EGFR as dominant heterodimerization partners determine a motogenic phenotype in human breast cancer cells", *FASEB J.*, **13**, 1939-1950, 1999.
3. K. Wiechen, S. Karaaslan, M. Dietel, "Involvement of the c-erbB-2 oncogene product in the EGF-induced cell motility of SK-OV-3 ovarian cancer cells", *Int. J. Cancer*, **83**, 409-14, 1999.
4. K. S. R. Spencer, D. Graus-Porta, J. Leng, N. Hynes, R. L. Klemke, " ErbB2 is necessary for induction of carcinoma cell invasion by ErbB family receptor tyrosine kinases", *J. Cell. Biol.*, **148**, 385-397, 2000.
5. F. Rossi, C. A. Charlton, and H. M. Blau "Monitoring protein-protein interactions in intact eukaryotic cells by β-galactosidase complementation", *Proc. Natl. Acad. Sci. U S A*, **94**, 8405-8410, 1997.
6. B. T. Blakely, F. M. Rossi, B. Tillotson, M. Palmer, A. Estelles, H. M. Blau **"**Epidermal growth factor receptor dimerization monitored in live cells", *Nat. Biotechnol*. **18**, 218-22, 2000.
7. J. N. Pelletier, F.-X. Campbell-Valois, and S. W. Michnick, "Oligomerization domain-directed reassembly of active dihydrofolate reductase from rationally designed fragments", *Proc. Natl. Acad. Sci. U S A*, **95**, 12141-12146, 1998.
8. I. Remy, I. A. Wilson, S. W. Michnick, "Erythropoietin receptor activation by a ligand induced conformation change", *Science*, **283**, 990-993, 1999.
9. C. Berney, G. Danuser, "FRET or no FRET: a quantative comparison", *Biophys. J.*, **84**, 3992-4010, 2003.
10. T. W. J. Gadella, T. M. Jovin, "Oligomerization of epidermal growth factor receptors on A431 cells studied by time-resolved fluorescence imaging microscopy. A stereochemical model for tyrosine kinase receptor activation", *J Cell Biol.*, **129**, 1543-58, 1995.
11. P. Nagy, G. Vereb, Z. Sebestyen, G. Horvath, S. J. Lockett, S. Damjanovich, J. W. Park, T. M. Jovin, J. Szollosi**, "**Lipid rafts and the local density of ErbB proteins influence the biological role of homo- and heteroassociations of ErbB2", *J Cell Sci*., **115**, 4251-62, 2002.

12. P. Nagy, L. Bene, M. Balazs, W.C. Hyun, S. J. Lockett, N. Y. Chiang, F. Waldman, B. G. Feuerstein, S. Damjanovich, J. Szollosi, "EGF-induced redistribution of erbB2 on breast tumor cells: flow and image cytometric energy transfer measurements", *Cytometry*, **32,** 120-131, 1998.
13. A. A. Deniz, M. Dahan, J. R. Grunwell, T. Ha, A. E. Faulhaber, D. S. Chemla, S. Weiss, P. G. Schultz, **"**Single-pair fluorescence resonance energy transfer on freely diffusing molecules: observation of Forster distance dependence and subpopulations", *Proc. Natl. Acad. Sci. U S A*; **96**, 3670-5, 1999.
14. A. A. Deniz, T. A. Laurence, G. S. Beligere, M. Dahan, A. B. Martin, D. S. Chemla, P. E. Dawson, P. G. Schultz, S. Weiss, "Single-molecule protein folding: diffusion fluorescence resonance energy transfer studies of the denaturation of chymotrypsin inhibitor 2", *Proc. Natl. Acad. Sci. U S A*; **97**, 5179-84, 2000.
15. S. Weiss**,** Fluorescence spectroscopy of single biomolecules, *Science*, **283**, 1676-83, 1999.
16. G. J. Schutz, W. Trabesinger, T. Schmidt**, "**Direct observation of ligand colocalization on individual receptor molecules", *Biophys J*., **74**, 2223-6, 1998.
17. L. Cognet, G. S. Harms, G. A. Blab, P. H. M. Lommerse, T. Schmidt, "Simultaneous dual-color and dual-polarization imaging of single", *Appl. Phys. Lett*., **77**, 4052-54, 2000.
18. B. S. Hendriks, L. K. Opresko, H. S. Wiley, D.Luffenburger,."Quantitative analysis of HER2-mediated effects on HER2 and epidermal growth factor receptor endocytosis: distribution of homo- and heterodimers depends on relative HER2 levels", *J Biol Chem*., **278**, 23343-23351, 2003.
19. B. S. Hendriks, L. K. Opresko, H. S. Wiley, D.Luffenburger, "Coregulation of epidermal growth factor receptor/human epidermal growth factorreceptor 2 (HER2) levels and locations: quantitative analysis of HER2overexpression effects", *Cancer Res.*, **63**, 1130-1137, 2003.
20. K. M. Ferguson, M. B. Berger, J. M. Mendrola, H. S. Cho, D. J. Leahy, M. A. Lemmon, "EGF activates its receptor by removing interactions that autoinhibit ectodomaindimerization", *Mol Cell*., **11**, 507-17, 2003.
21. T. P. Garrett, N. M. McKern, M. Lou, T. C. Elleman, T. E. Adams, G. O. Lovrecz, .M. Kofler, R. N. Jorissen, E. C. Nice, A. W. Burgess, C. W. Ward, "The crystal structure of a truncated ErbB2 ectodomain reveals an active conformation, poised to interact with other ErbB receptors", *Mol Cell*., **11**, 495-505, 2003.
22. T. P. Garrett, N. M. McKern, M. Lou, T. C. Elleman, T. E. Adams, G. O. Lovrecz, H. J. Zhu, F. Walker, M. J. Frenkel, P. A. Hoyne, R. N. Jorissen, E. C. Nice, A. W. Burgess, C. W. Ward, "Crystal structure of a truncated epidermal growth factor receptor extracellular domain bound to transforming growth factor alpha", *Cell*, **110**, 763-73, 2002.
23. H. S. Cho, K. Mason, K. X. Ramyar, A. M. Stanley, S. B. Gabelli, D. W. Jr. Denney, D. J. Leahy, "Structure of the extracellular region of HER2 alone and in complex with theHerceptin Fab", *Nature*, **421**, 756-60, 2003.
24. H. Ogiso, R. Ishitani, O. Nureki, S. Fukai, M. Yamanaka, J. H. Kim, K. Saito, A. Sakamoto, M. Inoue, M. Shirouzu, S. Yokoyama, "Crystal structure of the complex of human epidermal growth factor and receptorextracellular domains", *Cell*, **110**, 775-87, 2002.